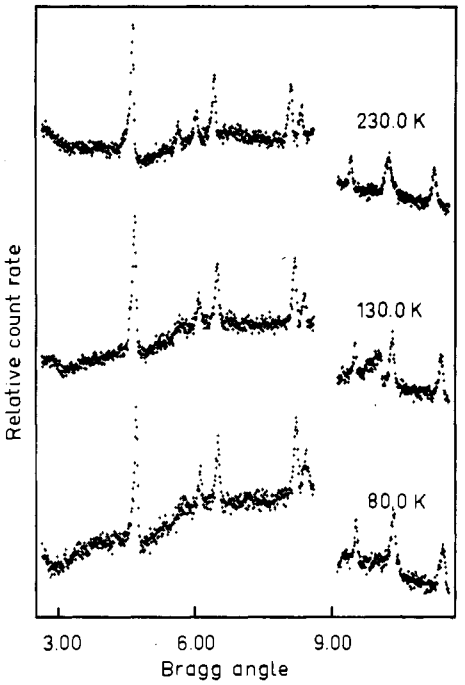

Figure 4. X-ray powder diffraction for $Co(H_2fsa_2en)(4\text{-}t\text{-}Bupy)_2$ over the temperature interval 230.0–80.0 K for decreasing temperatures.

regions in the diffraction angle range where the observed changes are particularly marked. It is clearly seen that, in the transition region, the individual patterns for the HS and LS states replace each other as the transition progresses. This observation is in agreement with the first-order character of the transition[7] and conforms to the general behavior of discontinuous spin-state transitions in compounds of iron(II).[4] According to Figure 3, the transition temperatures for the actual sample as determined on the basis of magnetic measurements are $T_c^{\downarrow}$ = 114 K and $T_c^{\uparrow}$ = 136 K. The value of $T_c^{\uparrow}$ is somewhat different from that published earlier,[7] which is not surprising since spin-state characteristics are known to be generally dependent on the solid-state properties of the sample.[4] A much larger discrepancy is shown by the hysteresis derived from I_{HS}/I_{tot} values of the X-ray diffraction data, which lead to the apparent transition temperatures $T_c^{\downarrow} \simeq 85$ K and $T_c^{\uparrow} \simeq 126$ K. This discrepancy is certainly too large to be attributed to differences of calibration of the temperature readings. It should be noted that the I_{HS}/I_{tot} values employed in the figure are based on the peak at 12.30°; cf. Figure 2. Most other major diffraction peaks show too much overlap with neighboring lines such that even a decomposition into Gaussians does not provide reliable values for the intensity of an individual line. This fact could introduce some uncertainty of I_{HS}/I_{tot} values, although a larger shift of the transition temperature is difficult to visualize. In particular, inspection of Figures 1 and 2 clearly demonstrates that the most conspicuous change of diffraction pattern occurs between 122.0 and 130.0 K. The difference between the hysteresis loop derived from X-ray diffraction and that obtained on the basis of magnetic data rather resembles the hysteresis differences found for some other spin-transition compounds, such as $[Fe(4,7\text{-}(CH_3)_2\text{-}phen)_2(NCS)_2]\cdot{}^1/_2(\alpha\text{-picoline})$[9] and $[Fe(3\text{-}OCH_3\text{-}SalEen)_2]PF_6$,[10] as the result of intensive grinding of the sample. Although the compounds in the present study were used as obtained, cycling of temperature could break the crystallites into smaller fragments. The effect expected for this situation[9] is similar to that of grinding[9,10] or the application of pressure,[7,11] i.e. a more gradual appearance of the transition, increased n_{HS} values at low temperatures due to a more incomplete transformation of spin state, and a lowering of the temperature where n_{HS} = 0.50, i.e. of the apparent transition temperatures $T_c^{\uparrow}$ and $T_c^{\downarrow}$. This is indeed what is observed for the results of Figure 3.

A single-crystal X-ray diffraction study of $Co(H_2fsa_2en)(py)_2$ in the HS state has been recently carried out.[12] According to this study, the cobalt(II) ion is in a distorted octahedral environment with an apical metal–donor atom bond length of 2.262 Å and a mean equatorial bond length of 2.079 Å. The comparison of structural data for various square-pyramidal HS and LS cobalt(II) compounds indicates[13] an overall bond length change of 0.09 Å. This is significantly smaller than the change normally accompanying a spin change in iron(II) (~0.18 Å).[6] The average change for equatorial Co–N bonds has been found as ≃0.15–0.21 Å, and that for equatorial Co–O bonds, as 0.04–0.07 Å. Recent EXAFS measurements performed at 295 and 40 K arrived at average bond length changes of 0.09 and 0.12 Å for the spin-state transitions in $Co(H_2fsa_2en)(H_2O)_2$ and $Co(H_2fsa_2en)(py)_2$, respectively.[13] It should be noted that the ΔS = 1 spin-state change in cobalt(II) involves only a single electron ($t_{2g}^6e_g^1 \leftrightarrow t_{2g}^5e_g^2$). Consequently, the metal–ligand bond length variation and the observable change of powder diffraction are expected to be generally smaller than for complexes of iron(II) or iron(III).

For $Co(H_2fsa_2en)(4\text{-}t\text{-}Bupy)_2$, the X-ray powder diffraction has been measured for a number of temperatures between 230.0 and 80.0 K. As is evident from Figure 4, no major change of the resulting pattern due to the variation of temperature is apparent, not even in the transition region. It has been verified on the basis of magnetic susceptibility measurements performed on the same sample that the transition takes place at $T_c^{\downarrow}$ = 136.5 K for decreasing and at $T_c^{\uparrow}$ = 150 K for increasing temperature. The values of the transition temperature show a slight difference from the values published previously.[8] The absence of any observable change in the X-ray powder diffraction for this compound on spin-state transition is surprising. However, it should be noted that many individual reflections of the crystallites may at least partly overlap, and thus the variation expected for HS and LS states could easily be concealed under the relatively broad powder peaks.

Acknowledgment. The authors appreciate financial support from the Deutsche Forschungsgemeinschaft, Bonn, West Germany. Critical reading of the manuscript by H. A. Goodwin, Sydney, is gratefully acknowledged.

Registry No. $Co(H_2fsa_2en)(py)_2$, 70995-74-3; $Co(H_2fsa_2en)(4\text{-}t\text{-}Bupy)_2$, 102109-99-9.

(9) König, E.; Ritter, G.; Kulshreshtha, S. K.; Csatary, N. *Inorg. Chem.* **1984**, *23*, 1903.
(10) Haddad, M. S.; Federer, W. D.; Lynch, M. W.; Hendrickson, D. N. *Inorg. Chem.* **1981**, *20*, 131.
(11) König, E.; Ritter, G.; Waigel, J.; Goodwin, H. A. *J. Chem. Phys.* **1985**, *83*, 3055.
(12) Charpin, P.; Nierlich, M.; Vigner, D.; Lance, M.; Thuéry, P.; Zarembowitch, J.; d'Yvoire, F. *J. Crystallogr. Spectrosc. Res.* **1988**, *18*, 429.1.
(13) Thuéry, P.; Zarembowitch, J.; Michalowicz, A.; Kahn, O. *Inorg. Chem.* **1987**, *26*, 851.

Contribution from the Department of Chemistry, Metcalf Center for Science and Engineering, Boston University, Boston, Massachusetts 02215

Applications of the Quantitative Analysis of Ligand Effects (QALE). Steric Profiles for Reactions Involving "Spectator" Phosphorus(III) Ligands

Klaas Eriks,* Warren P. Giering,* Hong-Ye Liu, and Alfred Prock*

Received November 23, 1988

"Spectator" phosphorus(III) ligands of organometallic complexes do not directly participate in chemistry at a metal center. Since spectator ligands remain in the coordination sphere of the metal, they influence the energies of the ground- and transition-state energies through transmission of their stereo–electronic properties to the metal center. Transition-metal reactions where

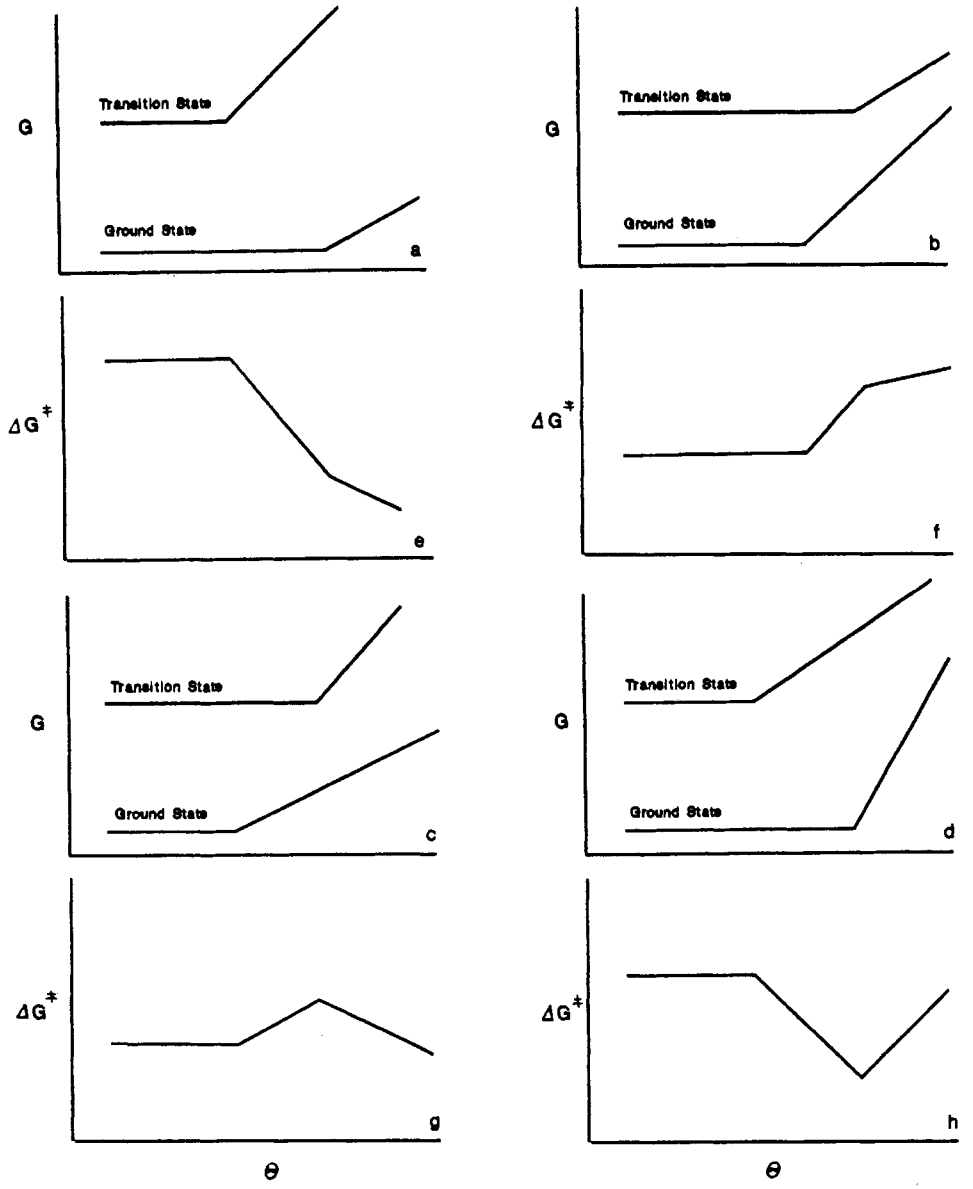

Figure 1. Idealized representations (a–d) of the variations of the ground- and transition-state free energies (G) as a function of the size (cone angle, θ) of electronically equivalent "spectator" phosphorus(III) ligands and expected steric profiles (plots of $-\Delta G^{\ddagger}$ versus θ) (e–h) for combinations of ground- and transition-state energies: (a, e) ground state is less congested and more flexible than the transition state; (b, f) ground state is more congested and less flexible; (c, g) ground state is more congested and more flexible; (d, h) ground state is less congested and less flexible.

phosphorus(III) ligands serve as spectator ligands may be collected into three general catagories: (1) dissociative, (2) associative, and (3) interchange reactions.[1]

QALE (quantitative analysis of ligand effects[2-7]) analysis of reactions involving spectator phosphorus(III) ligands predicts four steric profiles, the shapes of which depend on the relative congestion and flexibility[2] of the ground and transition states. The QALE method rests on the premises that the free energy of activation is divisible into steric (log k_{st}) and electronic (log k_{el}) components such that

$$\log k = \log k_{el} + \log k_{st} \qquad (1)$$

and that there are different thresholds for the onset of steric effects in the ground and transition states. Analysis of kinetic data is accomplished through construction of electronic and steric profiles. An electronic profile is a plot of log k for a series of isosteric ligands (or small ligands that do not exhibit steric effects) versus a measure of the σ-donicity (σ_d) of the phosphorus(III) ligands. The half-wave neutralization potentials[5] or related pK_a values[2,3] of HPR_3^+ have been frequently employed as measures of σ_d. More recently, we demonstrated[4] that the χ values[8] (Table I) for the trialkyl-, mixed alkyl/aryl-, and triarylphosphines are also good measures of σ_d when restricted to the aforementioned ligands.

log k_{st} is the difference between data points for other ligands and the electronic profile (at the same χ). The steric profile is generated by plotting log k_{st} versus the cone angle (θ) of the ligand. This is illustrated in Figure 2a,b.

The shape of the steric profile is a result of different responses of the ground and transition states to variations in the size of the spectator phosphorus(III) ligands. In considering how the phosphorus(III) ligands influence the rates of reaction, it is necessary to compare the ground and transition states in terms of congestion and flexibility. A more congested state will have a lower steric threshold. The energy of a less flexible state will

(1) Taube, H. *Comments Inorg. Chem.* **1981**, *1*, 17–31.
(2) Golovin, N. G.; Rahman, Md. M.; Belmonte, J. E.; Giering, W. P. *Organometallics* **1985**, *4*, 1981–91.
(3) Rahman, Md. M.; Liu, H.-Y.; Prock, A.; Giering, W. P. *Organometallics* **1987**, *6*, 650–8.
(4) Rahman, Md. M.; Liu, H.-Y.; Eriks, K.; Prock, A.; Giering, W. P. *Organometallics*, in press.
(5) Dahlinger, K.; Falcone, F.; Poe, A. J. *Inorg. Chem.* **1986**, *25*, 2654.
(6) Brodie, N. M.; Chen, L.; Poe, A. J. *Int. J. Chem. Kinet.* **1988**, *20*, 467–91.
(7) Poe, A. J. *Pure Appl. Chem.* **1988**, *60*, 1209–16.

(8) The χ values are defined as A_1 ν_{CO} (cm^{-1}) − 2056.1 cm^{-1} for $LNi(CO)_3$ (see ref 12).

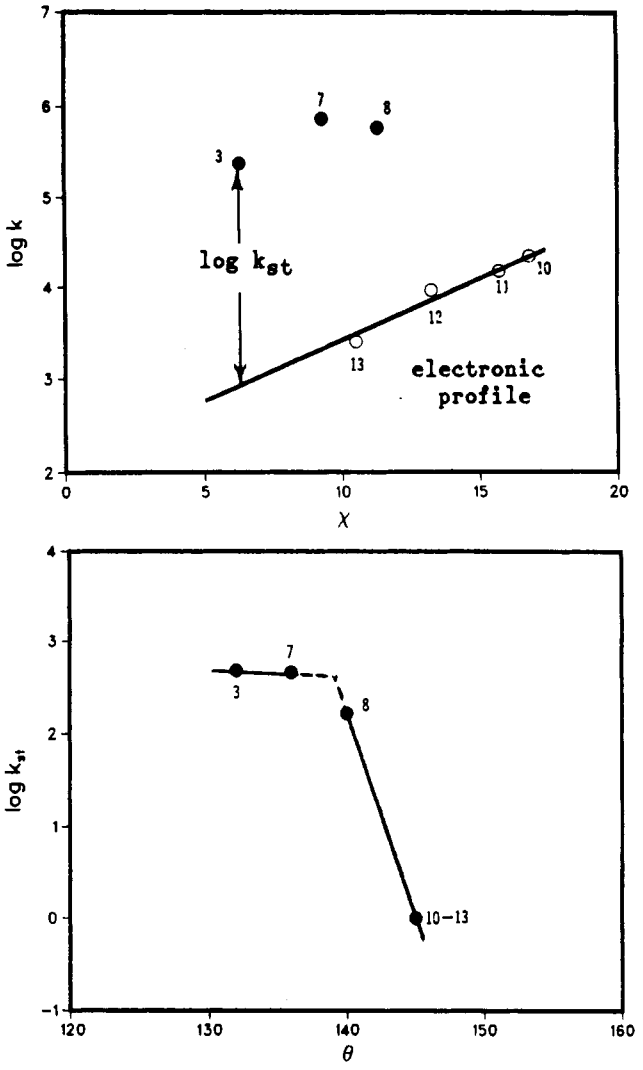

Figure 2. (a, Top) Electronic profile (plot of log k versus χ) for reaction 2. The line is drawn through points (open circles) for the isosteric (θ = 145°) ligands P(p-XPh)$_3$. Data are taken from ref 8. (b, Bottom) Steric profile for reaction 2 (plot of the deviation of data from the electronic profile shown in (a) versus the cone angle (θ) of the phosphorus(III) ligands). All appropriate kinetic data for reactions 2–4 and the stereoelectronic properties of the phosphorus(III) ligands are displayed in Table I. The intersections of the components of the steric profile are represented as dashed lines since we do not know the degree of curvature[6] in the region of the steric thresholds.

rise more rapidly than that of a more flexible state after the onset of steric effects. Figure 1a–d shows idealized plots of free energy versus size (θ) of electronically equivalent phosphorus(III) ligands for the four possible combinations of ground- and transition-state energies with different steric thresholds and flexibilities. Relative to the transition state, the ground states are sterically less congested and more flexible (Figure 1a), more congested and less flexible (Figure 1b), more congested and more flexible (Figure 1c), and less congested and less flexible (Figure 1d). The corresponding idealized steric profiles ($-\Delta G$ versus cone angle, θ; Figure 1e–h) are drawn below each free energy plot. Real examples (Figures 2b, 3, and 4b) of steric profiles (Figure 1e–g) were derived from QALE analyses of data drawn from the literature.[9-11]

(9) Herrick, R. S.; Peters, C. H.; Duff, R. R. *Inorg. Chem.* **1988**, *27*, 2214–9.
(10) Chalk, K. L.; Pomeroy, R. K. *Inorg. Chem.* **1984**, *23*, 444–9. In our original QALE analysis,[3] we employed pK_a values of HPR_3^+ for the construction of the electronic profile for this reaction. In this updated analysis, we used the χ values. The slope of the electronic profile for the isosteric ligands, P(p-XPh)$_3$ is almost zero. The results are virtually identical with our earlier analysis of these data.
(11) Liesing, R. A.; Ohman, J. S.; Takeuchi, K. J. *Inorg. Chem.* **1988**, *27*, 3804.

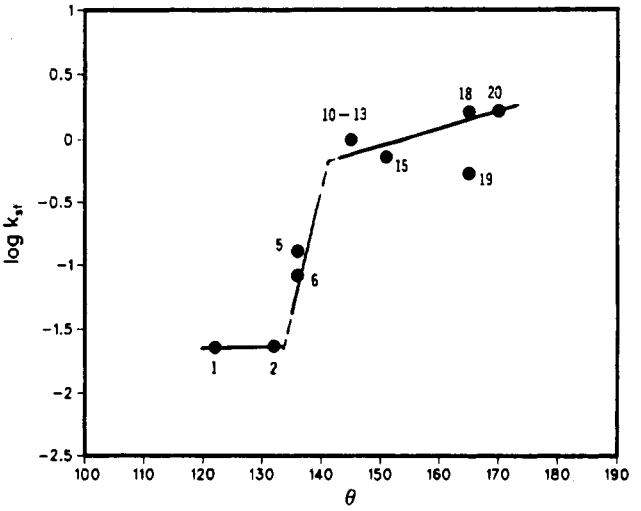

Figure 3. Steric profile for reaction 3. The analysis was originally described in ref 3 with data taken from ref 10.

The first idealized steric profile (Figure 1e) is consistent with an associative (addition) reaction where the coordination number of the transition state is higher than that of the ground state. In this model, the transition state is more congested and less flexible than the ground state. The steric profile (Figure 2b) for the addition of CO to $Mo(CO)_2(PR_3)Br_2$ is illustrative. The kinetic data for this second-order reaction were reported recently by Herrick.[9]

$$Mo(CO)_2(PR_3)_2Br_2 + CO \rightarrow Mo(CO)_3(PR_3)_2Br_2 \quad (2)$$

For ligands with small cone angles ($\theta < 139°$) there is no steric inhibition of the reaction. At 139°, there is a steric threshold that must correspond to the onset of steric effects in the more congested transition state of the reaction. After the steric threshold the transition state is destabilized relative to the ground state and the rate of the reaction drops rapidly.

The steric dependence of the system described by Figure 1b,f is that expected for a purely dissociative process. The departing ligand produces a transition state less congested and more flexible than the ground state. Our previously reported QALE analysis[3] of the data of Chalk and Pomeroy[10] for reaction 3 illustrates the

$$mer\text{-}Ru(CO)_3(SiCl_3)_2L + L' \rightarrow Ru(CO)_2(SiCl_3)_2LL' + CO \quad (3)$$

expected behavior. (The rate of reaction 3 is dependent only on the concentration of the complex and not the entering ligand, L'.) The steric profile (Figure 3) exhibits a threshold (θ = 135°) for the onset of steric effects in the ground state and another (θ = 140°) for the onset of steric effects in the transition state. Between these thresholds the rate of reaction rises very rapidly. After the second steric threshold, the energy of the transition state also rises and the rate of reaction appears to plateau. This leveling of the rate suggests that the flexibility of the transition state and ground state are similar; this seems reasonable since both are hexacoordinate with probably very similar structures.

The third type of steric profile (Figure 1g) is quite remarkable since it shows three very different regions of steric effects. At small cone angles there is no steric effect. This region is followed by a threshold for the onset of steric effects in the more congested ground state, which causes the rate of reaction to rise. The transition state of this model is less flexible than the ground state; hence, after the second steric threshold, the transition-state energy rises more rapidly than the ground-state energy. This results in an increase in the activation energy and a decrease in the rate of reaction. QALE analysis of the data reported by Takeuchi[11] for the entering ligand-dependent substitution of water by acetonitrile (AN) from $Ru(H_2O)(bpy)_2L^{2+}$ (reaction 4) provides a

$$cis\text{-}Ru(H_2O)(bpy)_2L^{2+} + AN \rightarrow cis\text{-}Ru(AN)(bpy)_2L^{2+} + H_2O \quad (4)$$

Table I. Stereo-Electronic Properties of Phosphorus(III) Ligands and Values of log k and log k_{st} for Reactions 2–4

				reacn 2[c]		reacn 3[c]		reacn 4[c]	
lig no.	lig	χ[a]	θ[b]	log k	log k_{st}	log k	log k_{st}	log k	log k_{st}
1	PMe_2Ph	10.60	122			−4.72	−1.64		
2	$P(allyl)_3$	10.30	132			−4.68	−1.63		
3	PEt_3	6.30	132	5.38	2.68			−3.08	−1.96
4	PPr_3	5.5	132					−3.00	−1.96
5	PBu_3	5.25	136			−3.85	−0.89	−2.54	−1.54
6	$PMePh_2$	12.10	136			−4.15	−1.08		
7	PEt_2Ph	9.30	136	5.86	2.66				
8	$PEtPh_2$	11.30	140	5.76	2.22				
9	$P(i\text{-}Bu)_3$	5.70	143					−0.54	0.58
10	$P(p\text{-}ClPh)_3$	16.80	145	4.34	0.0	−3.17	0.0		
11	$P(p\text{-}FPh)_3$	15.70	145	4.18	0.0	−3.12	0.0	−2.68	0.0
12	PPh_3	13.25	145	3.96	0.0	−3.05	0.0	−2.22	0.0
13	$P(p\text{-}MeOPh)_3$	10.5	145	3.40	0.0	−3.12	0.0	−1.96	0.0
14	$P(p\text{-}Me_2NPh)_3$	5.25	145					−0.096	0.0
15	$PPh_2(i\text{-}Pr)$	10.85	151			−3.19	−0.14		
16	$P(i\text{-}Pr)_3$	3.45	160					−0.74	−0.05
17	$PPh_2(o\text{-}MePh)$	12.75	161					−0.42	1.76
18	$P(m\text{-}MePh)_3$	11.1	165			−2.89	+0.21	−1.96	0.00
19	PBz_3	10.35	165			−3.20	−0.27	−0.78	1.06
20	$PPh_2(o\text{-}MeOPh)$	10.30	170			−2.83	+0.22		
21	PCy_3	1.40	170					−0.21	−0.14

[a] Data taken from or calculated with the data from ref 13 and 14. [b] Cone angle data taken from or calculated with the data found in ref 13. [c] log k and log k_{st} values for reactions 2–4 were calculated from data found in ref 9–11, respectively.

steric profile consistent with this model. This set of data is remarkable in that the largest steric acceleration of the reaction is observed for those ligands of intermediate size (i.e. $PPh_2(o\text{-}MePh)$, $\theta = 160°$) whereas smaller (PPh_3, $\theta = 145°$) and larger ($P(m\text{-}MePh)_3$, $\theta = 165°$; ref 10) ligands with comparable χ values exhibit diminished reactivity.[12] The steric profile (Figure 4b) shows a region where the rate of reaction increases with ligand size. (The region of no steric effect (see Figure 1g) apparently occurs for ligands with $\theta < 132°$ for which data were not taken.) A steric threshold near 154° ushers in steric effects in the transition state. Since the rate of reaction then decreases, the transition state must be less flexible than the ground state. The authors proposed that the reaction is an example of a dissociative-interchange (I_d) reaction where in the transition state the leaving group is largely dissociated and there is little bonding between the entering ligand and the metal. This QALE analysis supports their conclusions. The transition state is less congested than the ground state because the leaving group is largely dissociated and AN is just entering the coordination sphere. On the other hand, the flexibility of the transition state, as compared to the ground state, is decreased because of its greater coordination number. Intuitively, the steric profile in Figure 1g (and Figure 4b) is just what is expected for the I_d reaction, since at some point crowding about the complex must shut down the approach of the entering ligand and the reaction must cease.

We are not aware of a chemical example of the fourth type of steric profile (Figure 1h).

In conclusion, we have shown that sets of kinetic data for three different organometallic reactions in which phosphorus(III) ligands participate only as spectator ligands are readily interpreted in terms of the QALE model. QALE provides more detailed and useful interpretations of the ligand-effect data than are obtained by

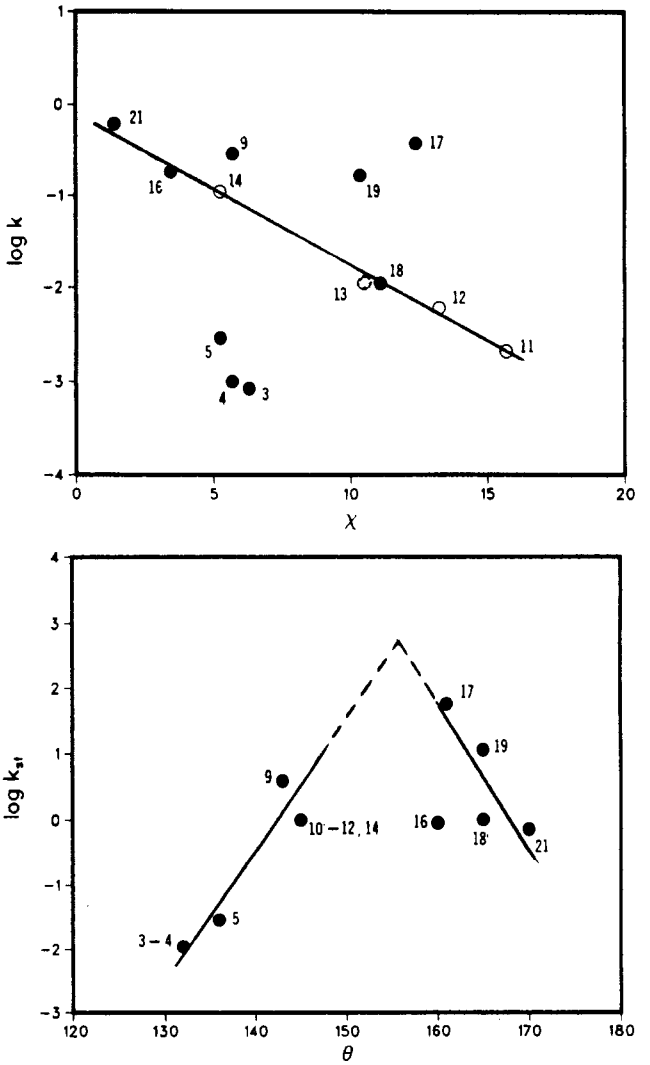

Figure 4. (a, Top) Electronic profile for reaction 4. The line is drawn through the isosteric ($\theta = 145°$) ligands $P(p\text{-}XPh)_3$ (open circles). Data are taken from ref 11. (b, Bottom) Steric profile for reaction 4.

(12) A reviewer suggested that we compare the analyses using the $E_{1/2}$ and χ values for *cis*-$Ru(H_2O)(bpy)_2L^{2+}$ of reaction 4 since $E_{1/2}$ values may be a more accurate measure of the electron density at the metal center than the χ values. Although this is often true, there are some serious pitfalls. The $E_{1/2}$ values measure the free energy difference between two states. If the stereo-electronic properties of these states differ, then the $E_{1/2}$ values will reflect these changes in addition to the intrinsic electron density at the metal center. This is clearly going on for these ruthenium complexes; for example, the complex containing the better electron donor ligand P(cyclohexyl)$_3$ is more difficult to oxidize than the complex containing PEt_3. This is probably attributable to increased congestion in the oxidized form. This phenomenon has been observed for the $E_{1/2}$ values for isonitrile complexes (Bohling, D. A.; Evans, J. F.; Mann, K. R. *Inorg. Chem.* **1982**, *21*, 3546–51).

(13) Tolman, C. A. *Chem. Rev.* **1977**, *77*, 313.
(14) Bartik, T.; Himmler, T.; Schulte, H.-G.; Seevogel, K. *J. Organomet. Chem.* **1984**, *272*, 29–41.

simple linear correlation with cone angle θ. Furthermore, these results provide strong support for the fundamental tenets of the QALE model: separation of energy of activation into electronic and steric components and the existence of steric thresholds in the ground and transition states. Because of the existence of different steric thresholds, it is very clear that there is no reason to expect a linear dependence of log k on the size of phosphorus(III) ligands except under very special circumstances.

Acknowledgment. We gratefully acknowledge the donors of the Petroleum Research Fund, administered by the American Chemical Society, and the Graduate School of Boston University for support of this work. We thank Professor Ronald Halterman (Boston University) for his helpful comments.

Contribution from the Department of Chemistry Education and Department of Chemistry, Seoul National University, Seoul 151, Korea

Synthesis, Characterization, and X-ray Structure of the Octahedral Nickel(II) Complex of a Pentadentate Hexaaza Macrobicyclic Ligand: Chloro(9-(methoxymethyl)-1,4,6,9,11,14-hexaazabicyclo-[12.2.1]heptadecane)nickel(II) Perchlorate

Myunghyun Paik Suh,* Jungwon Choi, Shin-Geol Kang, and Whanchul Shin

Received August 17, 1988

There are several pentadentate macrocyclic ligands and their complexes reported thus far.[1-15] The pentaaza macrocycles (L) containing a pyridine ring (**1–3**) were reported to form pentag-

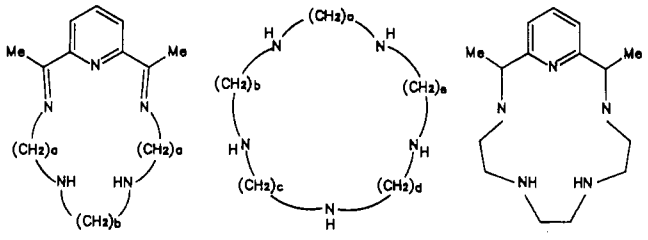

1; a = 2, b = 2 — 2; a = 2, b = 3 — 3; a = 3, b = 2

4; a = b = c = d = e = 2 — 5; a = 3, b = c = d = e = 2 — 6; a = c = d = 2, b = e = 3

7

onal-bipyramidal complexes $[MLX_2]^{n+}$ with Fe(III), Fe(II), or Mn(II) ions, where X stands for a monodentate ligand such as H_2O or NCS^-.[1-9] The Ni(II) complexes with pentaaza macrocyclic ligands **4–7** were reported to form distorted octahedral $[NiLX]^{n+}$ (X = Cl^- or H_2O, n = 1 or 2).[4,15] In this paper, we report a new Ni(II) complex with the hexaaza macrobicyclic ligand $C_{13}H_{30}N_6O$ that serves as a pentadentate ligand. The complex $[Ni(C_{13}H_{30}N_6O)Cl]ClO_4$ was synthesized by the simple template condensation reaction of polyamines with formaldehyde. The complex that has a distorted octahedral structure, contains a rarely observed four-membered chelate ring.

Experimental Section

Reagents. All chemicals and solvents used in the syntheses were of reagent grade and were used without purification. For the conductance and spectroscopic measurements, solvents were purified according to the literature method.[16]

Measurements. Infrared spectra were recorded with a Shimadzu IR-440 spectrophotometer. Conductance measurements were performed by using a Metrohm Herisau E518 conductometer and RC-216B_2 conductivity bridge. Electronic absorption spectra were obtained on a Perkin-Elmer Lambda 5 UV/vis spectrophotometer. Magnetic susceptibility was measured by the NMR method[17] on a Varian EM 360 60-MHz NMR spectrometer using a Wilmad 5-mm coaxial sample unit. For this measurement, Me_2SO and t-BuOH were used as the solvent and the reference material, respectively. Elemental analyses were performed by Galbraith Laboratories Inc., Knoxville, TN.

Table I. Crystallographic Data for $[Ni(C_{13}H_{30}N_6O)Cl]ClO_4$

$NiC_{13}H_{30}N_6O_5Cl_2$	space group $C2/c$ (No. 15)
fw = 480.02	T = 18 °C
a = 29.885 (13) Å	λ = 0.7107 Å
b = 9.838 (3) Å	ρ_{obsd} = 1.580 g cm^{-3}
c = 15.193 (5) Å	ρ_{calcd} = 1.592 g cm^{-3}
β = 109.89 (3)°	μ = 12.25 cm^{-1}
V = 4006 (3) Å^3	$R(F_o)$ = 0.049
Z = 8	$R_w(F_o)$ = 0.053

Table II. Atomic Coordinates (×10^4) and Equivalent Thermal Parameters (Å^2 × 10^3) of Non-Hydrogen Atoms for $[Ni(C_{13}H_{30}N_6O)Cl]ClO_4$

atom	x	y	z	U_{eq}[a]
Ni	3916.6 (0.2)	5891.7 (0.7)	3943.1 (0.4)	30
Cl	4578.8 (0.4)	4820 (2)	3643 (1)	46
N(1)	3594 (1)	4030 (5)	4250 (3)	38
C(2)	3925 (2)	2813 (7)	4584 (5)	52
C(3)	4168 (2)	3079 (8)	5620 (5)	57
N(4)	3894 (2)	4224 (6)	5875 (3)	48
C(5)	4137 (2)	5555 (8)	6092 (4)	50
N(6)	4313 (1)	6164 (5)	5355 (3)	35
C(7)	4426 (2)	7668 (7)	5541 (4)	47
C(8)	4543 (2)	8333 (8)	4746 (5)	54
N(9)	4160 (2)	8065 (5)	3833 (3)	46
C(10)	3695 (2)	8672 (7)	3783 (6)	55
N(11)	3396 (2)	7478 (5)	3887 (3)	39
C(12)	2966 (2)	7263 (8)	3044 (5)	48
C(13)	3098 (2)	6622 (8)	2256 (4)	50
N(14)	3476 (2)	5536 (5)	2569 (3)	39
C(15)	3306 (2)	4054 (7)	2532 (4)	49
C(16)	3182 (2)	3713 (8)	3398 (5)	49
C(17)	3445 (2)	4289 (7)	5084 (4)	43
C(18)	4320 (3)	8456 (10)	3072 (6)	80
O(19)	4400 (5)	10118 (12)	3297 (8)	70
O(19′)	4585 (4)	9522 (13)	2981 (10)	70
C(20)	4379 (5)	10761 (14)	2624 (11)	130
Cl(2)	3040 (1)	384 (2)	675 (1)	61
O(1)	2679 (3)	221 (12)	−145 (9)	269
O(2)	3404 (3)	−586 (7)	746 (6)	143
O(3)	3238 (2)	1764 (6)	684 (4)	101
O(4)	2922 (3)	209 (9)	1483 (6)	177

[a] $U_{eq} = {}^1/_3(\sum_i\sum_j U_{ij}a_i^*a_j^*a_ia_j)$.

(1) Nelson, S. M. *J. Chem. Soc., Dalton Trans.* **1979**, 1477.
(2) Margulis, T. N.; Zompa, L. J. *J. Chem. Soc., Chem. Commun.* **1979**, 430.
(3) Haque, Z. P.; Liles, D. C.; McPartlin, M.; Tasker, P. A. *Inorg. Chim. Acta* **1977**, *23*, L21.
(4) Rakowski, M. C.; Rycheck, M.; Busch, D. H. *Inorg. Chem.* **1975**, *14*, 1194.
(5) Fleisher, E.; Hawkinson, S. *J. Am. Chem. Soc.* **1967**, *89*, 720.
(6) Drew, M. G. B.; bin Othman, A. H.; McIlroy, P. D. A.; Nelson, S. M. *J. Chem. Soc., Dalton Trans.* **1975**, 2507.
(7) Drew, M. G. B.; bin Othman, A. H.; Hill, W. E.; McIlroy, P. D. A.; Nelson, S. M. *Inorg. Chim. Acta* **1975**, *12*, L25.
(8) Drew, M. G. B.; bin Othman, A. H.; McIlroy, P. D. A.; Nelson, S. M. *Acta Crystallogr., Sect. B; Struct. Crystallogr. Cryst. Chem.* **1976**, *B32*, 1029.
(9) Bishop, M. M.; Lewis, J.; O'Donoghue, T. D.; Raituby, P. *J. Chem. Soc., Chem. Commun.* **1978**, 476.
(10) Drew, M. G. B.; bin Othman, A. H.; McFall, S. G.; Nelson, S. M. *J. Chem. Soc., Chem. Commun.* **1977**, 558.
(11) Curry, J. D.; Busch, D. H. *J. Am. Chem. Soc.* **1964**, *86*, 592.
(12) Alexander, M. D.; Van Heuvelen, A.; Hamilton, H. G., Jr. *Inorg. Nucl. Chem. Lett.* **1970**, *6*, 445.
(13) Drew, M. G. B.; bin Othman, A. H.; McFall, S. G.; McIlroy, P. D. A.; Nelson, S. M. *J. Chem. Soc., Dalton Trans.* **1975**, 438.
(14) Drew, M. G. B.; Hollis, S. *Inorg. Chim. Acta* **1978**, *29*, L231.
(15) Fabbrizzi, L.; Micheloni, M.; Paoletti, P.; Poggi, A.; Lever, A. B. P. *J. Chem. Soc., Dalton Trans.* **1981**, 1438.
(16) Perrin, D. D.; Armarego, W. L. F.; Perrin, D. R. *Purification of Laboratory Chemicals*, 2nd ed.; Pergamon: Headington Hill Hall, Oxford, London, England, 1980.
(17) Evans, D. F. *J. Chem. Soc.* **1959**, 2003.

* To whom correspondence should be addressed at the Department of Chemistry Education, Seoul National University.

0020-1669/89/1328-1763$01.50/0